Estimation of the Interaction-Induced Effects on the Far-Infrared and Infrared Correlation Functions of HCl Dissolved in CCl_4: A Molecular Dynamics Study

George Chatzis and Jannis Samios*

Laboratory of Physical Chemistry, Department of Chemistry, University of Athens, Panepistimiopolis 15771, Athens, Greece

Received: April 26, 2001; In Final Form: August 16, 2001

The molecular dynamics simulation technique was used to study the interaction-induced dipole contributions to the dipole time correlation functions, related to the far-infrared and infrared absorption spectra of HCl dissolved in CCl_4 at liquid densities. The simulations presented here were based on an accurate effective potentia1 model which was described in a previous treatment of this solution. The "dipole-induced dipole" as well as the "back-induced dipole", as interaction-induction mechanisms between solute and solvents, were applied in order to calculate the induced dipoles of the species in the solution. The simulated dipole time correlation functions and spectral line shapes for far-infrared and infrared were compared with corresponding available experimental results and reasonable agreement was observed. It is found that the well-known interaction-induced dipole effects contribute insignificantly to the infrared, whereas they are not negligible in the case of the far-infrared absorption profile.

1. Introduction

Solutions of small polar molecules in polar or neutral solvents are among the systems for which the relative importance of the intermolecular interactions of different natures governing the solute dynamics still remains debatable. Note that solutions of hydrohalogens, and, in particular, those of hydrogen chloride (HCl) in nonpolar solvents, are representative solutions of such systems which have also received much attention from the experimentalists. To the best of our knowledge, far-infrared (FIR) and infrared (IR) spectroscopic techniques have been widely used by several authors[1−7] who studied the rotational dynamics of HCl dissolved in CCl_4. Still, some questions remain open as one attempts to elucidate spectral features of the system at different thermodynamic conditions. In general, these spectral features reflect the influence of specific molecular interactions upon the HCl/solute dynamics.

In two previous studies of HCl and DCl in CCl_4,[8,9] we have employed the molecular dynamics (MD) simulation technique in order to investigate the structural, thermodynamical, and single molecule dynamical properties of the system. The isotopic and temperature-dependent properties of the system have been also explored, and our results[9] are found to be in good agreement with the corresponding experimental data. Furthermore, previous treatments performed on systems ranging from pure simple liquids to liquid mixtures showed that computer simulation (CS) techniques have been successful in checking assumptions often used in theories of condensed phase spectroscopy. This computational approach is central in the present study. One aims to investigate the well-known interaction-induced effects on the total dipole moment time correlation functions (CFs), which are related to the FIR and IR absorption spectra of HCl in CCl_4. Consequently, the computer simulation results reported here may be regarded as an extension of our previous computational studies of the solution under investigation.

In the course of the present MD simulations, we have evaluated the permanent and electrostatic induced dipole contributions to the total dipole CFs of the system corresponding to the far-IR and IR absorption spectra. The calculations were carried out at thermodynamic conditions for which the experimental spectral profiles of the solution available in the literature do not show isolated rotational quantum absorption lines. In that particular case, a typical atomistic simulation of the system, such as the classical MD simulation technique, is an alternative approach to obtain directly the total dipole moment time CF of the solution as well as the corresponding absorption spectral line shape (via Fourier transform). It must be mentioned that the classical MD technique has been widely used in earlier theoretical treatments where the spectroscopic properties of a series of pure liquids and liquid mixtures[10−14] were treated.

In the following section, we present a summary of our theoretical considerations and assumptions introduced in the simulation to study the influence of the interaction-induced phenomena upon the FIR and IR absorption spectral line shapes of HCl diluted in CCl_4. Finally, the MD predictions of this study, in conjunction with the corresponding experimental data, are outlined and discussed.

2. Theoretical Background

Far-Infrared (FIR). The absorption coefficient per unit path length at cycle frequency ω and temperature T in the FIR, $\alpha(\omega)$, can be obtained either from the golden rule of quantum perturbation theory[15] or from the theory of linear response.[16] In any case, $\alpha(\omega)$ is connected with the Fourier transform (FT) of the system's total dipole moment CF, $C_M(t)$, according to the following relation:

$$\alpha(\omega) = \frac{4\pi n\omega}{3\hbar\eta(\omega)D(\omega)c}\tanh\left(\frac{\hbar\omega}{2k_BT}\right)\{\mathrm{Re}\}\{\int_0^\infty e^{i\omega t}C_M(t)\,dt\} \quad (1)$$

$n = (1/V)$ is the number density and $\eta(\omega)$ is the frequency

* To whom correspondence should be addressed. E-mail: isamios@cc.uoa.gr.

10.1021/jp011602n CCC: $20.00
Published on Web 09/25/2001

dependent refractive index of the sample. $D(\omega)$ denotes a frequency dependent internal field correction. By assuming that the product $\eta(\omega)D(\omega)$ is equal to one,[17] one is lead to conclude that the shape of the absorption spectrum is mainly dominated by the time dependence of the CF $C_M(t)$, i.e.

$$C_M(t) = \langle \vec{M}_{tot}(0) \cdot \vec{M}_{tot}(t) \rangle \quad (2)$$

The evaluation of the total dipole moment at time t, $\vec{M}_{tot}(t)$, is based upon theoretical considerations for the total permanent dipole moment, $\vec{M}_P$, of the probe diatomic molecules and the total induced-dipole moment, $\vec{M}_I$,[18−20] of all of the species in the solution:

$$\vec{M}_{tot}(t) = \vec{M}_P(t) + \vec{M}_I(t) \quad (3)$$

For our diluted mixture of a certain mole fraction, the total number of molecules, N, contains N_A (A = CCl_4) solvents and N_B (B = HCl) solutes.

The total permanent dipole moment at time t of the system, $\vec{M}_P(t)$, can be calculated by summing all of the orientationally dependent permanent dipoles of the HCl solutes, $\vec{\mu}_i^P(t)$:

$$\vec{M}_P(t) = \sum_{i=1}^{N_B} \vec{\mu}_i^P(t) \quad (4)$$

Even though the evaluation of $\vec{M}_P(t)$ is a simple task, the corresponding total induced dipole moment, $\vec{M}_I(t)$, needs to be evaluated in a considerably more complicated fashion.

This means that, for a given configuration of the system under investigation, one will have to assume that the quantity $\vec{M}_I(t)$ can be expressed as the sum of the induced dipole moments, $\vec{\mu}_{ij}(t)$:

$$\vec{M}_I(t) = \sum_{i \neq j} \sum \vec{\mu}_{ij}(t) \quad (5)$$

where $\vec{\mu}_{ij}$ denotes the dipole moment that the pair of molecules i and j induce at each other via a given induction mechanism. Moreover, from eq 5a, the sum $\sum_j \vec{\mu}_{ij}$

$$\vec{\mu}_{I,i} = \sum_j \vec{\mu}_{ij}(t) \quad (5a)$$

determines the total induced dipole moment of the molecule i, $\vec{\mu}_{I,i}(t)$, at time t. It should be noted that the time evolution of the molecular quantity $\vec{\mu}_{I,i}(t)$ contains information about (a) the relative translational motion of the reference molecule i with respect to the motion of its neighboring molecules, (b) its reorientation in the laboratory frame of reference, and (c) the time dependent fluctuations of its cage molecules.

We have indeed evaluated the collective total induced dipole moment, $\vec{M}_I(t)$, of the system on the basis of two suggested and distinct induction recipes, namely, the well-known first order " dipole−induced dipole" (DID) and the "back-induced dipole" (BID) schemes. According to the first one, each diatomic solute molecule j ($j = 1(1)N_B$) interacts with every other molecule i ($i = 1(1)N$, $i \neq j$) in the sample and induces a dipole $\vec{\mu}_{ij}(t)$ on it via an electrostatical polarization mechanism. Note that the DID mechanism employed in the present study requires the use of the electrostatic field gradient arising due to the permanent dipole moment $\vec{\mu}_i^P(t)$ of the HCl molecules. By analogy to the former mechanism, the BID induction scheme has been applied as follows. The resulting induced dipole moment on each solvent molecule, $\vec{\mu}_{I,i}^{DID}(t)$ ($i = 1(1)N_A$), induces back a dipole on each of the other molecules (HCl or CCl_4) in the sample. Generally, the BID is a many body effect. However, according to our definition, it is only a three-body effect.

It must be emphasized that, in the present treatment, only long-ranged induction mechanisms among the molecules in the sample have been considered. Short and intermediate range induced dipole contributions, due to the overlap exchange, repulsion, distortion, and field gradient effects, have been neglected. It has been also assumed that the four body induced dipoles and higher order terms, contribute insignificantly to the induced part of the system's total dipole moment. Furthermore, the induced dipole contributions due to the solvent−solvent polarization effects as results of the octupole or higher order multipole moments arising among CCl_4 molecules[21] have been ignored.

On the basis of the above considerations, the total induced dipole moment of the system, $\vec{M}_I$, can be split into a sum of two terms as follows:

$$\vec{M}_I(t) = \vec{M}_I^{CCl_4}(t) + \vec{M}_I^{HCl}(t) \quad (6)$$

$\vec{M}_I^{CCl_4}(t)$ and $\vec{M}_I^{HCl}(t)$ are given by means of the following equations

$$\vec{M}_I^{CCl_4}(t) = \sum_{i=1}^{N_A} \vec{\mu}_{I,i}^{CCl_4}(t) \quad (6a)$$

$$\vec{M}_I^{HCl}(t) = \sum_{i=1}^{N_B} \vec{\mu}_{I,i}^{HCl}(t) \quad (6b)$$

where $\vec{\mu}_{I,i}^{CCl_4}(t)$ and $\vec{\mu}_{I,i}^{HCl}(t)$ denotes the calculated total induced dipole moment of each CCl_4 and HCl molecule in the sample, respectively.

By using the separation procedure of eq 3, the total dipole moment CF $C_M(t)$ given in eq 2 may be expressed as a sum of four different CFs:

$$\begin{aligned} C_M(t) = \langle (\vec{M}_P(0) + \vec{M}_I(0)) \cdot (\vec{M}_P(t) + \vec{M}_I(t)) \rangle = \\ \langle \vec{M}_P(0) \cdot \vec{M}_P(t) \rangle + \langle \vec{M}_I(0) \cdot \vec{M}_I(t) \rangle + \langle \vec{M}_P(0) \cdot \vec{M}_I(t) \rangle + \\ \langle \vec{M}_I(0) \cdot \vec{M}_P(t) \rangle = C_M^{PP}(t) + C_M^{II}(t) + C_M^{PI}(t) + C_M^{IP}(t) = \\ C_M^{PP}(t) + C_M^{II}(t) + C_M^{+}(t) \end{aligned} \quad (7)$$

$C_M^{PP}(t)$ and $C_M^{II}(t)$ represents the autocorellation function of the total permanent and induced dipole moment in the sample, respectively. $C_M^{PI}(t)$ and $C_M^{IP}(t)$, or the sum of them, $C_M^{+}(t)$, describe the interference between the total permanent and the total induced dipole moments of the sample.

As mentioned above, according to the first-order DID formalism employed in the present study, for the calculation of the induced dipole of a molecule in the solution due to a solute one requires the existence of an induction mechanism among the two species. In our treatment, this mechanism was based on the first leading electric multipole moment of HCl, that is, its permanent dipole moment. Higher order multipole terms of the solute, such as the quadrupoler ones, etc, have been ignored because the HCl molecule exhibits a relatively large permanent dipole moment of about 1.08−1.28 D.[22,23] Additionally, the calculation of the dipole induced dipoles and back induced dipoles of the molecules was based upon an isotropic polarizability of the solvent ($\alpha^{CCl_4} = 11.2$ Å^3 [22]) and an anisotropic polarizability of the axially symmetric solute molecule. The data used in our calculation for the isotropic, $\alpha^{HCl} = 2.60$ Å^3, and

the anisotropic, $\gamma^{HCl} = 0.311$ Å^3, component of the polarizability of HCl were borrowed from the literature.[22,23]

In what follows, we will first describe in detail the employed interaction-induced procedure. Thus, according to the first-order DID mechanism, the electric field originated by the permanent dipole moment of the solute molecule j, $\vec{\mu}_j^{\,p}$, at the center of mass of another solute or solvent molecule i can be expressed as

$$\vec{E}_{ij}^{DID} = T_{ij}^{(2)}(R_{ij})\cdot\vec{\mu}_j^{\,p} \tag{8}$$

where the second rank tensor $T_{ij}^{(2)}$ is built up by the second-order gradient of the reciprocal center of mass separation vector R_{ij} between the pair of particles i and j. In Cartesian coordinates, the explicit form of the tensor $T_{ij}^{(2)}$ is

$$\nabla_\alpha\nabla_\beta\left(\frac{1}{R_{ij}}\right) = \frac{1}{R_{ij}^{\,5}}(3R_{ij,\alpha}R_{ij,\beta} - R_{ij}^{\,2}\delta_\alpha\beta) \tag{9}$$

(α,β,γ) denote the Cartesian components (x,y,z) and $\delta_{\alpha\beta}$ is the Knonecker $\delta-$ function.

By denoting $\hat{u}_j(t)$ the unitary vector in the direction of the permanent dipole moment along the molecular axis of the HCl molecule j, the explicit expression for the latter vector, $\vec{\mu}_j^{\,p}(t)$, in Cartesian coordinates, is given by means of eq 10

$$\mu_{j,\alpha}^{p}(t) = \mu_{HCl}^{p}\cdot u_{j,\alpha}(t) \tag{10}$$

where the greek indices α denotes the $x-$, $y-$, $z-$ direction, respectively.

According to eqs 9 and 10, eq 8 takes the form

$$E_{ij,\alpha}^{DID} = \frac{\mu_{HCl}^{p}}{R_{ij}^{\,5}}[3(\hat{u}_j\cdot\vec{R}_{ij})R_{ij,\alpha} - R_{ij}^{\,2}u_{j,\alpha}] \tag{11}$$

Thus, the induced dipole moment on each molecule is obtained by means of the following equation

$$\vec{\mu}_{ij}^{DID}(t) = \hat{\alpha}_i(t)\cdot\vec{E}_{ij}^{DID}(t) \tag{12}$$

where $\hat{\alpha}_i$ is the polarizability tensor of the ith molecule. Note that, in the case of the CCl_4 molecule, the first order in the polarizability tensor was used, because for the molecular symmetry T_d the polarizability is isotropic (i.e., scalar). Albeit some authors calculate the induced dipole moment $\vec{\mu}_{ij}^{DID}$ of the ith linear molecule by analyzing its polarizability into the isotropic and anisotropic part, we choose in the first instance to evaluate[24] its total induced dipole moment, $\vec{\mu}_{I,i}^{DID}$, as follows: Concretely, the first step toward solving this problem is to obtain the total induced electric field of the molecule by using eqs 11 and 13:

$$\vec{E}_i^{DID}(t) = \sum_j \vec{E}_{ij}^{DID}(t) \tag{13}$$

Additionally, we calculate the two total electric field components, namely the parallel, $\vec{E}_i^{DID,||}$, and the normal, $\vec{E}_i^{DID,\perp}$, to the molecular axis of the HCl molecule, according to the following relations:

$$[(\vec{E}_i^{DID}\cdot\hat{u}_i)\hat{u}_i] = \vec{E}_i^{DID,||} \tag{14a}$$

$$(\vec{E}_i^{DID} - \vec{E}_i^{DID,||}) = \vec{E}_i^{DID,\perp} \tag{14b}$$

In the second step of our procedure, the expected total DID moment, $\vec{\mu}_{I,i}^{DID}$, of the molecule is obtained via the well-known relations

$$\vec{\mu}_{I,i}^{DID,||} = \alpha_i^{||}\cdot\vec{E}_i^{DID,||} \tag{15a}$$

$$\vec{\mu}_{I,i}^{DID,\perp} = \alpha_i^{\perp}\cdot\vec{E}_i^{DID,\perp} \tag{15b}$$

$$\vec{\mu}_{I,i}^{DID} = \vec{\mu}_{I,i}^{DID,||} + \vec{\mu}_{I,i}^{DID,\perp} \tag{16}$$

$\alpha_i^{||}$, $\alpha_i^{\perp}$ denote the parallel and the normal to the molecular axis of HCl components of the polarizability, respectively. Certainly

$$\alpha_i^{HCl} = \frac{1}{3}(\alpha_i^{||} + 2\alpha^{\perp}) \tag{17a}$$

$$\gamma_i^{HCl} = \alpha_i^{||} - \alpha_i^{\perp} \tag{17b}$$

Finally, according to the BID mechanism the total induced dipole moment on each solvent molecule, $\vec{\mu}_{I,i}^{DID}$ $(i = 1(1)N_A)$, induces back a dipole moment on each of the other molecules in the sample. Thus, the resulting induced dipole moment on each molecule, $\vec{\mu}_{I,i} \equiv \vec{\mu}_{I,i}^{CCl_4}$ or $\vec{\mu}_{I,i}^{HCl}$, may be simply calculated as the sum of two terms, the contributions due to the DID and the BID induction mechanism.

As we can see below, the aforementioned interaction-induced computational procedure provides valuable information regarding the influence of the interaction induced-dipole moment contributions to the IR CF, $C_{IR}(t)$, and the corresponding spectral line shape of the polar diatomic dissolved in the non polar CCl_4.

Infrared. According to the above theoretical considerations, the related to the IR absorption total dipole moment of a probe solute molecule, $\vec{\mu}_{tot,i}^{HCl}$, is constituted by its permanent dipole, $\vec{\mu}_i^{\,p}$, and the parallel component to the molecular axis, $\vec{\mu}_{I,i}^{||}$, of its total induced dipole moment $\vec{\mu}_{I,i}$

$$\vec{\mu}_{tot,i}^{HCl}(t) = \vec{\mu}_i^{\,p}(t) + \vec{\mu}_{I,i}^{||}(t) \tag{18}$$

Following the well-known procedure outlined in ref 25, the IR dipole CF may be written as follows:

$$C_{IR}(t) = \left|\frac{\partial\vec{\mu}_{tot,i}^{HCl}}{\partial q_l}\right| \langle\hat{v}_i(0)\cdot\hat{v}_i(t)\rangle \tag{19}$$

Here, $\hat{v}_i(t)$ denotes the unit vector of the total dipole moment, $\vec{\mu}_{tot,i}^{HCl}(t)$, of the solute molecule i given by eq 18. In general, the direction of the vector $\vec{\mu}_{tot,i}^{HCl}(t)$ may be the same or opposite to that of the permanent dipole $\vec{\mu}_i^{\,p}(t)$ of the solute. It depends, however, on the strength and the direction of the induced dipole component, $\vec{\mu}_{I,i}^{||}$, of the solute with respect to its permanent dipole moment. Specifically, from the pertinent results presented herein it can be seen that the average magnitude of $\vec{\mu}_{I,i}^{||}(t)$ of HCl is quite small when compared to its permanent dipole moment value. Thus, according to eq 18 the resulting total dipole moment, $\vec{\mu}_{tot,i}^{HCl}(t)$, and the permanent dipole, $\vec{\mu}_i^{\,p}(t)$, of a solute exhibit permanently the same direction. As we can see from the calculated CFs $C_{IR}(t)$ presented below, this result leads to the conclusion that the line shape of the IR absorption spectra of this solution is mainly due to the permanent dipole moment contribution of the solute molecules in the sample.

3. Results and Discussion

The calculated dipole moment CFs and the corresponding spectral line shapes presented here are based on NVE-MD

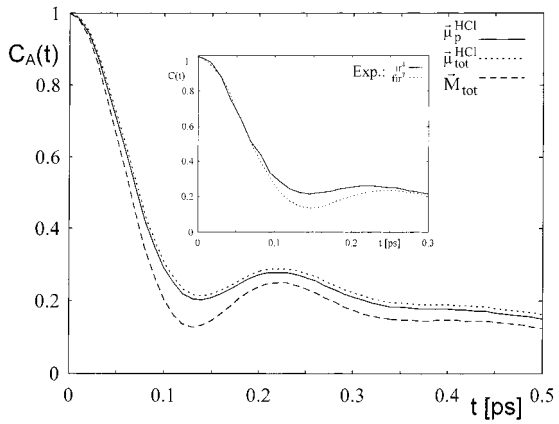

Figure 1. Comparison of the simulated dipole moment autocorellation functions (ACFs) of the diluted mixture HCl/CCl_4 at 290 K. The solid line (—) corresponds to the HCl molecule permanent dipole $\vec{\mu}_p^{HCl}$ ACF; the short dash (- - -) corresponds to the HCl total dipole moment $\vec{\mu}_{tot}^{HCl}$ ACF; and the long dash (— —) corresponds to the total dipole M_{tot} ACF of the sample.

simulations of two solutes in 254 solvents with the usual cubic periodic boundary conditions. The analytical description of the employed potential model has been determined in our previous simulation study.[8] Most of the fundamental technical details applied in the present simulations have been described in our previous MD studies[8,9] of the same solution. We notice that, for a given configuration of the system, the interaction-induced dipoles among the molecules have been calculated for center of mass intermolecular separations, R_{ij}, fulfilling the condition $R_{ij} < L/2$, where L denotes the length of the simulation box. Finally, it should be mentioned that, after equilibration, each MD run has been extended up to 150 ps and the pertinent dipole time CFs were obtained using the usual method of the direct calculation (DC).

Dipole Moment CFs. The three dipole moment time CFs of interest

$$C_A(t) = \langle \vec{A}(0)\cdot\vec{A}(t)\rangle, \quad \vec{M}_{tot}, \vec{\mu}_i^p, \vec{\mu}_{tot,i}^{HCl} \tag{20}$$

were obtained at three different temperatures (273, 290, and 343 K) and at solvent densities corresponding to the orthobaric pressures.

In all cases, the time dependent quantities $\vec{M}_{tot}$ and $\vec{\mu}_{tot,i}^{HCl}$ were calculated at each time step of the simulation by means of eqs 3 and 18, respectively. Moreover, as mentioned in the previous section, $\vec{\mu}_i^p(t)$ denotes the orientation of the time dependent permanent dipole vector of the ith HCl molecule, obtained at each time step in the simulation run. Note that each CF, $C_A(t)$, was obtained in time intervals of five time steps (5 $\delta t = 0.01$ps) over a large total time interval and for a large number of time origins. It was also checked that with the used number of solutes and solvents ($N_B/N_A = 2/254$) and the cutoff radius of $L/2$, the contribution of more distant molecules to the interaction-induced total dipole moment of the system, $\vec{M}_I$, is negligibly small. This result is supported by an supplementary MD simulation of four solutes dissolved in 496 solvents at 290 K.

In what follows, we will first discuss the results obtained for the above-mentioned dipole CFs in conjunction with data from prior FIR and IR experimental studies of the mixture under investigation. Thus, the computed CFs, $C_A(t)$, at 290 K are shown in Figure 1. Note that the three dipole CFs are normalized to their own amplitudes at $t = 0$. The insert figure illustrates the experimental IR (see Figure 4 in ref 4 and Figure 4a in ref 8) and FIR (see Figure 2 in ref 7) corresponding dipole CFs of this highly diluted solution at room temperature.

Let us first investigate the behavior of the experimental curves seen in Figure 1. Thus, the time evaluation of both CFs confirms that the qualitative trends observed in the IR dipole CF are also observed in the corresponding correlation obtained using the FIR technique. However, a closer inspection of these two experimental CFs indicates clearly the existence of some systematic difference between them. Specifically, the two curves practically overlap each other at very short times and up to $t \cong 0.08$ps. Afterward, each curve exhibits a positive minimum followed by a submaximum and converges to zero after relatively long time. Note also that the IR CF goes through a shallower positive minimum than the FIR function. In addition, the positive hump in the IR CF is located at shorter time and shifted to a slight higher ordinate value compared to that in the FIR correlation. We mention here that the question of whether the IR and FIR band shapes in the case of dilute solutions give essentially the same information about the rotational motion of the solute molecules in the sample has been a matter of considerable research in the past. A general conclusion which may be drawn from that previous research is the following. The IR band shape of a vibrational transition with the transition moment in the direction of the permanent dipole moment provides the same single-solute CF as the FIR dipolar absorption of a dilute solution if the effects due to vibrational relaxation, rotation−vibration coupling, and the well-known interaction induced-dipoles on the spectral line shapes are negligible or eliminated in some way. We recall here that Ikawa et al. in ref 7 pointed out that the feature of the experimental FIR $C(t)$ for HCl in CCl_4 is in good agreement with that obtained from the IR band.[1] However, contrary to that expectation, the direct comparison among the FIR[7] and the most recent available experimental IR[4] data CFs (see Figure 1) reveals that the feature of the FIR CF is in semiquantitative agreement with that from the IR band of HCl in CCl_4 at comparable thermodynamical conditions. The main question we would like to address here is, "What is the underlying microscopic mechanism which is responsible for the behavior of the experimental far-IR CF to be somewhat different compared to that of the IR function". To explain the above-mentioned observations, it is convenient to inspect the simulated CFs, $C_A(t)$, in conjunction to the experimental curves. The MD results for the three dipole CFs are depicted in Figure 1 up to 0.5 ps. As we can see, the two first-order Legendre reorientational CFs of the solute molecules ($C_A(t)$, A $\equiv \vec{\mu}_i^p$ and $\vec{\mu}_{tot,i}^{HCl}$) exhibit quantitatively a quite similar behavior in going from one curve to another. A comprehensive and convincing explanation for this result is given below. As mentioned in section 3, the direction of the vector $\vec{\mu}_{tot,i}^{HCl}(t)$ (see eq 18) may be the same or not to that of the permanent dipole, $\vec{\mu}_i^p(t)$, of the solute. According to eq 18, it depends from the vector $\vec{\mu}_{1,i}^{||}(t)$ of the solute with respect to the vector $\vec{\mu}_i^p(t)$. Note, however, that the average strength of $\vec{\mu}_{1,i}^{||}(t)$ has been found to be quite small in comparison to the corresponding permanent dipole moment. This result leads to the conclusion that both $\vec{\mu}_{tot,i}^{HCl}(t)$ and $\vec{\mu}_i^p(t)$ reveal the same direction at any time. Moreover, the overall behavior of each of these two correlations is found to be in quite good accordance with the corresponding IR experimental CF. Note that the calculated experimental $C_{IR}(t)$ CFs obtained from previous IR studies were compared and discussed in our previous study of this system.[8,9] Thus, our MD results support the suggestion made in previous experimental studies[1,4,5] that the IR absorption band shape of HCl in

CCl_4 is not affected by the well-known interaction induced dipole effects among the species in the solution.

Let us for the moment concentrate on the behavior of the experimental and simulated FIR corresponding dipole moment CFs shown in Figure 1. As it can be seen, the time evolution of the experimental FIR CF is fairly well reproduced by the MD collective total dipole moment correlation $C_M(t)$. At very short times, the $C_M(t)$ decreases faster than the aforementioned $C_{IR}(t)$ correlations. Also, $C_M(t)$ exhibits a deeper positive minimum than the $C_{IR}(t)$ curves. It is of course due to different orientation of the total dipole moment of the sample $\vec{M}(t)$ compared to that of $\vec{\mu}_i^{p}(t)$ and $\vec{\mu}_{tot,i}^{HCl}(t)$. Summing up, it appears that the interaction-induced dipole effects are not negligible in the case of the FIR absorption line shape of this solution. In this particular case, it is very interesting to compare our FIR results for the HCl/CCl_4 system with previous published theoretical ones for similar mixtures obtained by other groups. We mention, e.g., the far-IR absorption of the diluted mixtures of HCl, DCl dissolved in liquefied inert gases (Ar, Kr, and Xe) and liquid SF_6, which have been investigated theoretically[26] (see also ref 17−19 in ref 26). These studies have shown that the induced contributions must be considered in order to reproduce the FIR experimental absorption spectrum of such systems, especially at high densities. This result is in accordance with our findings presented in this work.

Another point of particular interest here is to examine the temperature dependence of the simulated $C_A(t)$ ($A \equiv \vec{\mu}_i^{p}$ and $\vec{M}_{tot}$) CFs. The results obtained for these correlations at 273, 290, and 343 K are displayed in Figure 2 parts a−c. As we can see from Figure 2, the two $C_A(t)$ curves become nearly superimposed with increasing temperature. This MD result appears to be in agreement to what is expected in this particular case. Again, this illustrates the fact that at higher temperatures or lower densities, the strength of the interaction-induced effects is weak compared to lower temperatures. In other words, a slight modification of the molecular cage around the solute molecule seems to be very important for the behavior of these CFs.

Figure 3a shows the behavior of the calculated $C_A(t)$ ($A \equiv \vec{\mu}_{tot}^{HCl}$) CF at 273 and 343 K. At very short times, both curves follow the well-known behavior of the free rotor. Also, the initial decrease of $C_A(t)$ is more rapid at higher temperature, as expected. Generally, the $C_A(t)$ curves show a slower decay with decreasing temperature. It means that the reorientational motion of the solute is somewhat slowed with increasing density.

The IR absorption line shapes CFs of HCl in CC_4 corresponding to the simulated $C_A(t)$ ($A \equiv \vec{\mu}_{tot}^{HCl}$) are shown in Figure 3b. The aforementioned IR absorption spectra were estimated by Fourier transformation of these CFs at 273 and 343 K. Note also that these spectra are normalized to the same amplitude. We mention that the asymmetry in the simulated line shapes has been introduced by employing in our calculations the related Boltzmann factor between the P and R absorption intensities. The spectra show three absorption maxima, which will be designated as the usual P, Q, and R branches of the rotation−vibration absorption band of linear molecules, observed also in experiment. Eventually, we found that the line shapes of the simulated IR spectra are in quite good agreement with corresponding experimental[1,2,4] data.

The simulated total dipole moment CFs, $C_M(t)$, at 273 and 343 K are compared in Figure 4. These functions show a relatively similar temperature behavior to that obtained for the IR CFs discussed above. Unfortunately, temperature-dependent experimental FIR absorption spectra and corresponding CFs for HCl in CCl_4 are not available in the literature. Therefore, the reliability of the temperature dependence of the simulated FIR CFs obtained in the framework of the present study must be judged experimentally.

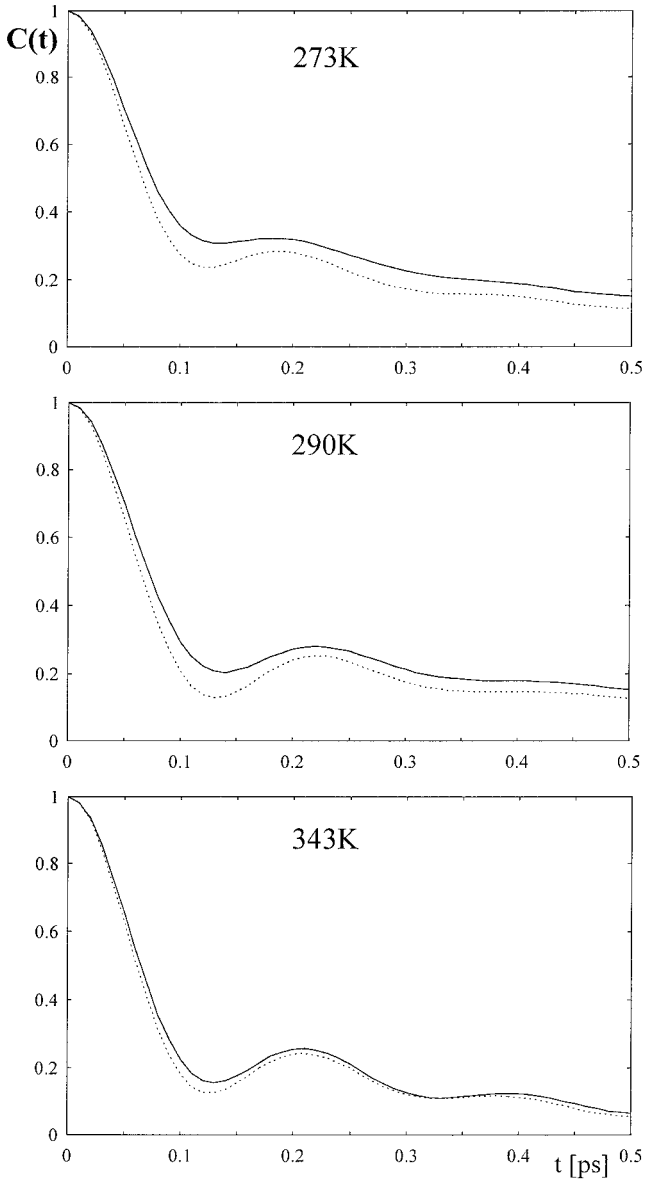

Figure 2. Permanent and induced dipole contributions to the total dipole moment ACFs with temperature. In any case, solid line (—) denotes the $\vec{\mu}_{tot}^{HCl}$ and the dashed line (- - -) the $\vec{M}_{tot}$ ACFs, respectively.

Finally, Figure 5 displays the simulated FIR absorption spectrum of the solution at 290 K in comparison with that of the corresponding experiment.[7] The calculated spectrum has been obtained by numerical Fourier transformation of the simulated total dipole moment CF $C_M(t)$ using eqs 1−3. To compare the calculated with the experimental spectrum profile, the absorption maximum of the calculated curve is set equal to that of the experimental one. By inspecting these curves, we see clearly that the simulated FIR spectrum profile is almost identical to the experimental one. This fact denotes the significance of the interaction induced contributions to the FIR absorption of the system.

4. Concluding Remarks

In the present article, the molecular dynamics simulation technique was employed to elucidate some spectral features of the diluted mixture of HCl in CCl_4. The simulations presented

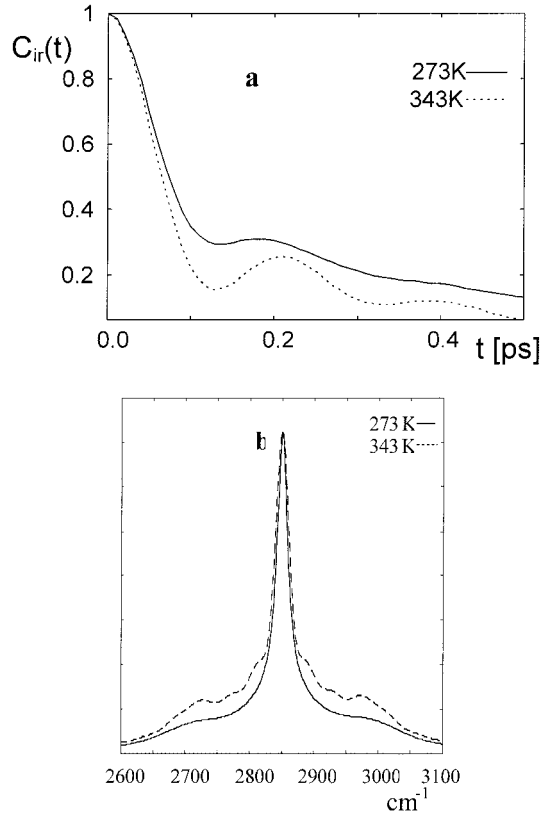

Figure 3. Temperature dependence of the IR corresponding ACFs and its reflection on the HCl spectrum.

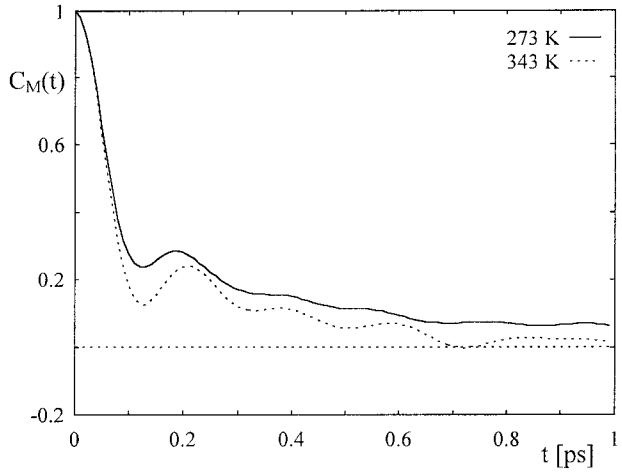

Figure 4. The temperature dependence of the $\vec{M}_{tot}$ ACFs.

here were carried out in the NVE statistical mechanical ensemble at temperatures of 273, 290, and 343 K and densities corresponding to the normal pressure. Also, all of the simulations of the system are based on an accurate effective potential model we have described and tested in two previous treatments of this highly diluted solution.

The main purpose of this work was to investigate systematically the permanent and electrostatical dipole-induced contributions to the IR and far-IR absorption spectra and corresponding correlation functions (CFs). To realize this, the collective total dipoles of the system were calculated by assuming two distinct induction mechanisms among the species in the sample, namely, the dipole-induced dipole as well as the back-induced dipole. Thus, the most interesting dipole CFs, corresponding to the IR and FIR absorption spectra, were calculated and found to be in good agreement with available experimental data. In this way,

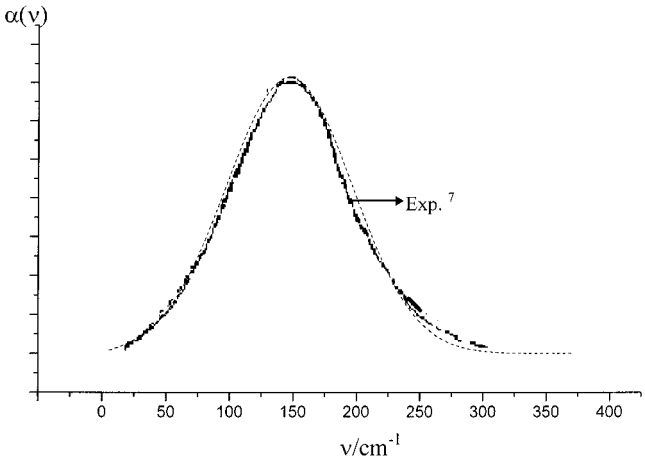

Figure 5. Comparison of the simulated with the corresponding experimental[7] fir absorption line shapes, $\alpha(\nu)$, at room temperature, normalized to the same amplitude.

it was possible to estimate the influence of the interaction induced effects on the formation of the IR and FIR spectra and CFs.

Finally, we found that the above-mentioned effects are not negligible in the case of FIR absorption profile, whereas they do not contribute to the IR absorption of this mixture, as expected.

Acknowledgment. This work was carried out within the Project No. 70/4/3394AU. The financial support of the University of Athens is gratefully acknowledged. The CPU time allocation on the machines of the Computing Center of the University of Athens-Greece is also gratefully acknowledged.

References and Notes

(1) Keller, B.; Knenbuehl, F. *Helv. Phys. Acta* **1972**, *45*, 1127.
(2) Lascombe, J.; Besnard, M.; Caloine, P. B.; Devaure, J.; Perrot, M. *Molecular Motion in Liquids*; Lascombe, J., Ed.; D. Reidel Publishing Co.: Dordrecht, Holland, 1974.
(3) Turrell, G. J. *Mol. Spectrosc.* **1978**, *19*, 383.
(4) Mushayakarara, E. C.; Turrell, G. *Mol. Phys.* **1982**, *46*, 991. Idrissi, A.; Arroume, M.; Turrell, G. *J. Mol. Struct.* **1993**, *294*, 103.
(5) Ohikubo, Y.; Ikawa, S.; Kimura, M. *Chem. Phys. Lett.* **1976**, *43*, 138.
(6) Ikawa, S.; Sato, K.; Kimura, M. *Chem. Phys.* **1980**, *47*, 65.
(7) Ikawa, S.; Yamazaki, S.; Kimura, M. *Chem. Phys.* **1980**, *51*, 151.
(8) Chatzis, G.; Chalaris, M.; Samios, J. *Chem. Phys.* **1998**, *228*, 241.
(9) Chatzis, G.; Samios, J. *Chem. Phys.* **2000**, 257, 51.
(10) Tildesley, D. J.; Madden, P. A. *Mol. Phys.* **1983**, *48*, 129.
(11) Müller, A.; Steele, W. A.; Versmold, H. J. *Chem. Phys.* **1993**, *99*, 4993.
(12) Samios, J.; Mittag, U. *J. Phys. Chem.* **1994**, *98*, 2033.
(13) Stassen, H.; Dorfmüller, Th.; Landanyi, B. M. J. *Chem. Phys.* **1994**, *100*, 6138.
(14) Medina, A.; Calvo Hernandez, A.; Roco, J. M. M.; Velasco, S. J. Mol. Liq. **1996**, *70*, 169. Medina, A.; Calvo Hernandez, A.; Velasco, S.; Guardia, E. J. *Chem. Phys.* **1994**, *100*, 252.
(15) McQuarrie, D. A. *Statistical Mechanics*; Harper & Row: New York, 1976.
(16) Brot, C. *Dielectric and Related Molecular Processes*; Davies, M., Ed.; Specialist Periodical Reports, The Chemical Society of London: London, 1975; Vol. 2, p 1.
(17) Lascombe, J.; Besnard, M. *Mol. Phys.* **1986**, *58*, 573.
(18) Buckingham, A. D. *Quart. Rev. Chem. Soc.* **1959**, *13*, 189.
(19) Buckingham, A. D. *Adv. Chem. Phys.* **1967**, *12*, 107.
(20) Bohr, J. F.; Hunt, K. L. C. *J. Chem. Phys.* **1987**, *87*, 3821.
(21) Dorfmüller, Th.; Samios, J.; Mittag, U. *Chem. Phys.* **1986**, *107*, 397.
(22) Gray, C. G.; Gubbins, K. E. *Theory of Molecular Fluids*; Oxford University Press: Oxford, U.K., 1984.
(23) Maroulis, G. J. *Chem. Phys.* **1998**, *108*, 5432.
(24) Samios, J.; Mittag, U.; Dorfmüller, Th. *Mol. Phys.* **1985**, *56*, 541.
(25) Dellis, D.; Samios, J. *Chem. Phys.* **1995**, *192*, 281.
(26) Roco, J. M. M.; Calvo Hernandez, A.; Velasco, S. *J. Chem. Phys.* **1995**, *103*, 9161.